SCIENTIFIC REPORTS

OPEN

SUBJECT AREAS:
ELECTROCATALYSIS
FUEL CELLS

Received
29 December 2014

Accepted
12 February 2015

Published
19 March 2015

Correspondence and requests for materials should be addressed to E.F.H. (holby@lanl.gov)

Activity of N-coordinated multi-metal-atom active site structures for Pt-free oxygen reduction reaction catalysis: Role of *OH ligands

Edward F. Holby[1] & Christopher D. Taylor[2,3]

[1]Los Alamos National Laboratory, Materials Science and Technology Division, Los Alamos, NM, 87545 USA, [2]DNV GL, Strategic Research & Innovation, Dublin, OH 43017 USA, [3]Fontana Corrosion Center, Dept. of Materials Science & Engineering, The Ohio State University, Columbus, OH 43210 USA.

We report calculated oxygen reduction reaction energy pathways on multi-metal-atom structures that have previously been shown to be thermodynamically favorable. We predict that such sites have the ability to spontaneously cleave the O_2 bond and then will proceed to over-bind reaction intermediates. In particular, the *OH bound state has lower energy than the final 2 H_2O state at positive potentials. Contrary to traditional surface catalysts, this *OH binding does not poison the multi-metal-atom site but acts as a modifying ligand that will spontaneously form in aqueous environments leading to new active sites that have higher catalytic activities. These *OH bound structures have the highest calculated activity to date.

Pt-free catalysts (PFCs) for the oxygen reduction reaction (ORR) promise to drastically reduce the cost of proton exchange fuel cells (PEFCs) for automotive and stationary power generation[1]. Recent improvements in the activity and durability of such catalysts has rekindled interest in these systems but lack of knowledge of the active site where the ORR occurs has limited the rational, bottom-up design of PFCs[2–4]. Insight regarding the structure of the ORR active site in PFCs would serve to guide synthesis by providing target structures. Maximizing the density of these target structures would lead to greatly improved catalysts, capable of replacing Pt in PEFC cathodes.

Computational studies have proven to be of great use in the rational design of catalyst structures[5,6]. A mature formalism for calculating ORR and oxygen evolution reaction (OER) pathways in acidic electrochemical environments has been developed over the previous decade, allowing for calculation of both relative structural stability as well as predicted structure-ORR activity relations[7–10]. This formalism, and its modifications in which non-canceling entropic, solvation, and zero-point energies are included, has been applied to a number of PFC active site structures[11–17] but predicted activities are significantly below what has been observed experimentally. In order to address this gap, different structures must be considered.

By treating active sites as Fe-N defects in a graphene host material, a number of structural motifs have been derived[18–20]. Several properties of these candidate active sites have been elucidated: 1) Fe incorporation is stabilized by nearest-neighbor coordination with N; 2) Fe-N defects are most stable at graphene edges: and 3) Fe-N edge defects are thermodynamically driven to form small clusters, constituting multi-metal-atom sites. These multi-metal-atom PFC sites have been suggested in a number of previous publications[21–23] but the thermodynamic basis for their existence has only recently been identified.

The multi-metal-atom aspect of the calculated structures can have an impact on the ORR reaction pathway, leading to a dissociative ORR pathway[20] instead of the associative pathways found in single-metal-atom sites[16]. A more detailed analysis of binding energies of ORR intermediates via use of the computational hydrogen electrode (CHE) methodology and density functional theory (DFT) has been used to calculate the maximum exergonic applied potential, V_{TH}, i.e., the maximum potential at which no thermodynamic (*TH*) barrier occurs in the calculated reaction pathway between neighboring intermediate states (see, for instance, Ref. 12). Potentials higher than the calculated V_{TH} have a thermodynamic barrier between intermediate reaction states. The difference between V_{TH} and the ORR reversible potential (1.23 V) represents a thermodynamic overpotential and thus, the closer V_{TH} is to the reversible potential, the higher the predicted activity of a given site. This formalism disregards

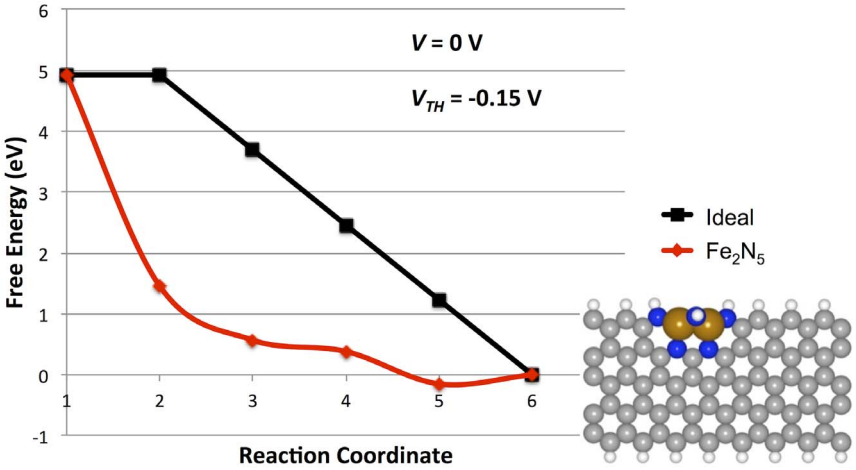

Figure 1 | Calculated ORR dissociative pathway potential energy surface for Fe_2N_5 edge structure (inset). Reaction coordinates correspond to the given systems: (1) O_2 +4 H^+ + 4 e^-, (2) *O + *O + 4 H^+ + 4 e^-, (3) *O + *OH + 3 H^+ + 3 e^-, (4) *O + 2 H^+ + 2 e^- + H_2O, (5) *OH + H^+ + e^- + H_2O, (6) * + 2 H_2O.

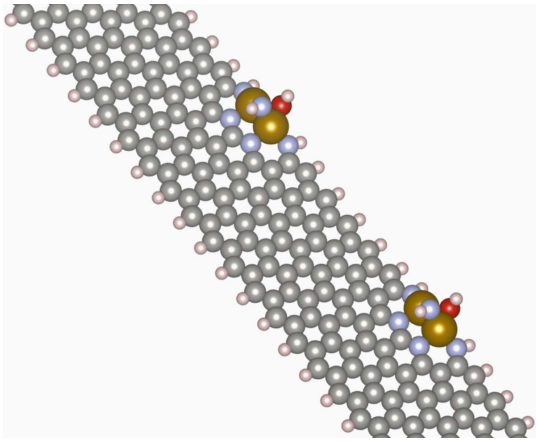

Figure 2 | Relaxed Fe_2N_5(*OH) edge structure showing locally minimized active site structure with bound *OH. Note that the site is not fully blocked, as is likely to occur in a typical surface catalyst, since the opposite side of the active site is still accessible to reactants.

kinetic barriers between intermediate states (as well as solvation and entropic effects) but is useful for comparing relative activities and predicting limiting steps in the ORR reaction pathway. Details of the DFT calculations can be found in the methods section.

The calculated reaction pathway for the multi-metal-atom Fe_2N_5 structure is shown in Figure 1. Due to the spontaneous dissociation of O_2, a dissociative pathway is assumed. It is readily apparent that the reaction pathway at 0 V potential is significantly lower than the ideal pathway, plotted in black, representing overbinding at all ORR intermediate steps. Due to the *OH bound state (reaction coordinate 5) being a lower energy than the ORR final state (2 H_2O molecules, reaction coordinate 6), the value of V_{TH} is −0.15 V, which indicates a very inactive ORR catalyst structure. We predict that the *OH bound state would spontaneously form in water bearing aqueous electrolytes and be persistent over a wide range of applied potentials.

In many heterogeneous catalyst systems, overbinding of *OH would be indicative of catalyst poisoning. The persistent *OH would serve to block active surface sites. The three-dimensional nature of the Fe_2N_5 site, however, means that even with a persistent *OH ligand, the active site is not sterically hindered from reacting further with an O_2 molecule. As shown in Figure 2, the *OH is found to bind at the graphene edge host and the bridging N tilts perpendicular to

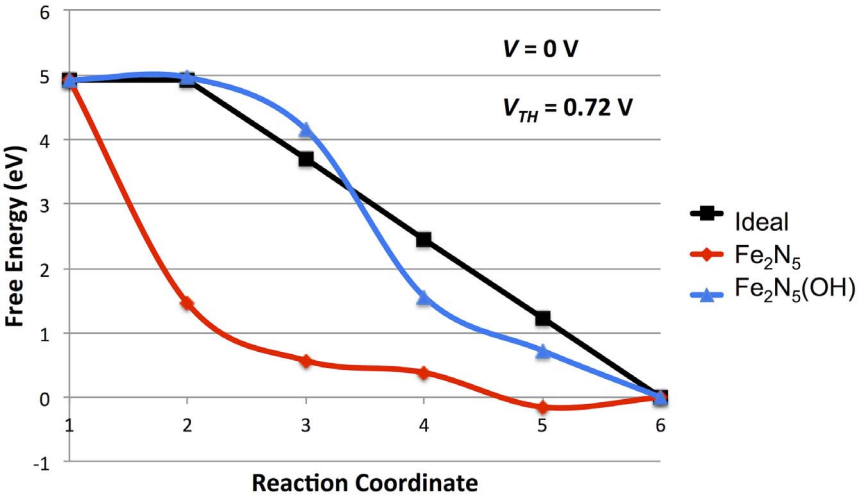

Figure 3 | Calculated ORR potential energy surfaces with and without *OH. Reaction coordinates for the Fe_2N_5 structure's dissociative pathway correspond to those of Figure 1. Reaction coordinates for the *OH bound structure correspond to the given systems: (1) O_2 +4 H^+ + 4 e^-, (2) *OO + 4 H^+ + 4 e^-, (3) *OOH + 3 H^+ + 3 e^-, (4) *O + 2 H^+ + 2 e^- + H_2O, (5) *OH + H^+ + e^- + H_2O, (6) * + 2 H_2O.

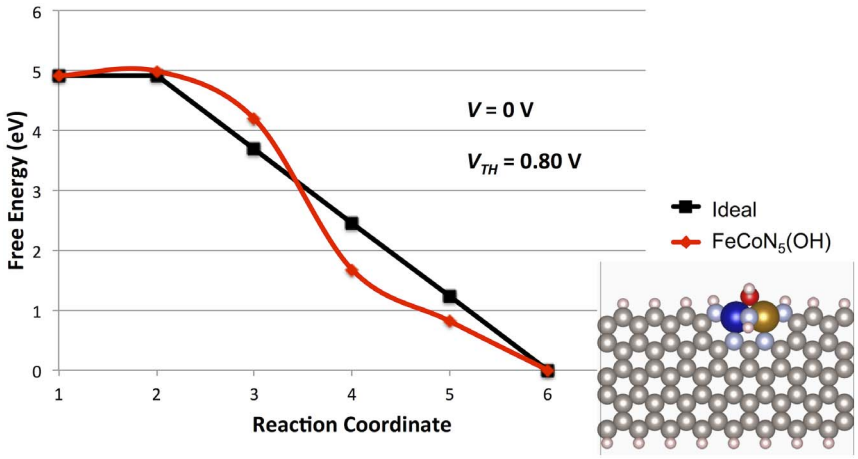

Figure 4 | Calculated ORR potential energy surface for mixed-multi-metal atom $FeCoN_5$ structure with *OH ligand. Reaction correspond to the given systems: (1) O_2 +4 H^+ + 4 e^-, (2) *OO + 4 H^+ + 4 e^-, (3) *OOH + 3 H^+ + 3 e^-, (4) *O + 2 H^+ + 2 e^- + H_2O, (5) *OH + H^+ + e^- + H_2O, (6) * + 2 H_2O. For all intermediates, adsorption on the Fe atom was lower energy than on the Co atom. The adsorbate free structure is shown as an inset.

the *OH. This leaves the side opposite the rotated N free to interact with O_2.

Treating the *OH bound Fe_2N_5 site as the thermodynamically stable site in water-bearing electrolytes, we have calculated the reaction pathway energetics as shown in Figure 3. The effect of the *OH ligand and the resulting increased coordination of the Fe atoms drastically increases the calculated activity, leading to a V_{TH} value of 0.72 V, an increase of 0.87 V versus the *OH free site. The potential determining step in this reaction pathway remains the final protonation step of the *OH intermediate. Additionally, the *OH ligand alters the O_2 binding such that spontaneous dissociation does not occur and so an associative ORR pathway becomes the more likely pathway.

Due to the multi-metal-atom nature of the predicted stable site, it is interesting to consider the effect of mixed-metal active site structures in similar structures. Such mixed-metal optimization adds an additional parameter that can be used to tune activity in multi-metal-atom sites. It has previously been shown that the combination of Fe and Co can alter catalyst activity in synthesized systems[2]. Exchanging one Fe for a Co atom in the previously considered high activity Fe_2N_5(*OH) site leads to an $FeCoN_5$(*OH) site structure. This structure and its calculated reaction pathway is shown in Figure 4. This structure has a calculated V_{TH} value of 0.80 V which is the highest calculated value for any PFC structure to date. The potential determining step in this pathway is the protonation of the *OO intermediate. While direct comparison to experimental data is hindered by mass-transport contributions, this predicted highest activity structure presents an attractive PFC synthesis target.

In summary, stability calculations suggest that spontaneous *OH ligand formation on multi-metal-atom N-coordinated PFC active site structures are thermodynamically likely to be formed during synthesis. Calculated reaction pathways suggest that such sites are significantly more ORR active than single-metal-atom or metal-free sites previously considered in the literature. While it is not possible to definitively say that the presented multi-metal-atom sites are responsible for the high activity found in current state-of-the art PFCs due to a lack of direct observation, these structures are attractive targets for rational design synthesis approaches. Further studies are required in order to include the roles of kinetic barriers between intermediate states, metal atom spin states, solvation of bound intermediates, and zero-point and entropic contributions specific to multi-metal-atom edge sites.

Methods

Spin-polarized periodic density functional theory (DFT) as implemented in the Vienna *ab initio* Simulation Package (*VASP*)[24–27] was used to calculate the relaxed atomic and electronic structure of the candidate active sites as well as intermediate structures for the potential energy surfaces. The GGA method as implemented by Perdew, Burke, and Ernzerhof (PBE-GGA)[28,29] was used to describe the exchange-correlation functional component of the Hamiltonian. An energy cut off of 400 eV was used for the plane-wave basis set. A convergence criteria for the electronic self-consistent loop of 10^{-5} eV was utilized and structures were relaxed until all forces were below 0.02 eV/Å. 8 × 5 carbon pair zig-zag graphene nanoribbons were used as the C-host material for the active sites and vacuum of at least 20 Å was used between periodic ribbons to limit self-interaction. Gamma-point centered 5 × 1 × 1 K-point meshes were used to sample the Brillouin zone with the 1 values corresponding to the two vacuum directions. van der Waals interactions are included in all calculations through the use of the DFT-D2 method of Grimme[30]. A variety of models exist in the literature to include zero-point energy, entropy, and solvation effects. Of particular interest is the work of Lyalin, *et al.*[31], as it includes the largely balancing effects of all three effects on a B-N surface. Unfortunately, a different reaction pathway than that considered in this work is considered. Szakacs, *et al.*[15], have interpreted these values for the associative pathway considered here and found the major contribution for the intermediate states to be destabilization of the *O + 2 H^+ + 2 e^- + H_2O state (Reaction Coordinate 4) by 0.40 eV. Addition of this term does not change the potential determining intermediate states that lead to V_{TH} for any of the three considered reaction pathways (Reaction Coordinates 5 → 6 and 2 → 3). Instead of adopting this potentially system and exchange-correlation functional dependent methodology, we assume full cancelation of these three effects and report pathways based solely on calculated binding energies from internal energies. This cancelation assumption has previously been shown a fair approximation for ORR intermediates on Pt surfaces[7,32]. Further justification of cancelation of ZPE, entropy, and solvation effects is the focus of future work.

1. Chen, Z., Higgins, D., Yu, A., Zhang, L. & Zhang, J. A review on non-precious metal electrocatalysts for PEM fuel cells. *Energy & Environmental Science* **4**, 3167–3192 (2011).
2. Wu, G., More, K. L., Johnston, C. M. & Zelenay, P. High-Performance Electrocatalysts for Oxygen Reduction Derived from Polyaniline, Iron, and Cobalt. *Science* **332**, 443–447 (2011).
3. Lefevre, M., Dodelet, J. P. & Bertrand, P. Molecular Oxygen Reduction in PEM Fuel Cells: Evidence for the Simultaneous Presence of Two Active Sites in Fe-Based Catalysts. *The Journal of Physical Chemistry B* **106**, 8705–8713 (2002).
4. Lefevre, M., Proietti, E., Jaouen, F. & Dodelet, J.-P. Iron-Based Catalysts with Improved Oxygen Reduction Activity in Polymer Electrolyte Fuel Cells. *Science* **324**, 71–74 (2009).
5. Norskov, J. K., Bligaard, T., Rossmeisl, J. & Christensen, C. H. Towards the computational design of solid catalysts. *Nat Chem* **1**, 37–46 (2009).
6. Curtarolo, S. *et al.* The high-throughput highway to computational materials design. *Nat Mater* **12**, 191–201 (2013).
7. Anderson, A. B. Insights into electrocatalysis. *Physical Chemistry Chemical Physics* **14**, 1330–1338 (2012).
8. Norskov, J. K. *et al.* Origin of the Overpotential for Oxygen Reduction at a Fuel-Cell Cathode. *Journal of Physical Chemistry B* **108**, 17886–17892 (2004).
9. Man, I. C. *et al.* Universality in Oxygen Evolution Electrocatalysis on Oxide Surfaces. *ChemCatChem* **3**, 1159–1165 (2011).
10. Koper, M. T. M. Thermodynamic theory of multi-electron transfer reactions: Implications for electrocatalysis. *Journal of Electroanalytical Chemistry* **660**, 254–260 (2011).
11. Zhang, P., Lian, J. S. & Jiang, Q. Potential dependent and structural selectivity of the oxygen reduction reaction on nitrogen-doped carbon nanotubes: a density

functional theory study. *Physical Chemistry Chemical Physics* **14**, 11715–11723 (2012).
12. Studt, F. The Oxygen Reduction Reaction on Nitrogen-Doped Graphene. *Catal Lett* **143**, 58–60 (2013).
13. Kattel, S., Atanassov, P. & Kiefer, B. Density Functional Theory Study of Ni_x/C Electrocatalyst for Oxygen Reduction in Alkaline and Acidic Media. *The Journal of Physical Chemistry C* **116**, 17378–17383 (2012).
14. Kattel, S., Atanassov, P. & Kiefer, B. Catalytic activity of Co-N_x/C electrocatalysts for oxygen reduction reaction: a density functional theory study. *Physical Chemistry Chemical Physics* **15**, 148–153 (2013).
15. Szakacs, C. E., Lefevre, M., Kramm, U. I., Dodelet, J.-P. & Vidal, F. A density functional theory study of catalytic sites for oxygen reduction in Fe/N/C catalysts used in H_2/O_2 fuel cells. *Physical Chemistry Chemical Physics* **16**, 13654–13661 (2014).
16. Calle-Vallejo, F., Martinez, J. I. & Rossmeisl, J. Density functional studies of functionalized graphitic materials with late transition metals for oxygen reduction reactions. *Physical Chemistry Chemical Physics* **13**, 15639–15643 (2011).
17. Kattel, S. & Wang, G. A density functional theory study of oxygen reduction reaction on Me-N4 (Me = Fe, Co, or Ni) clusters between graphitic pores. *Journal of Materials Chemistry A* **1**, 10790–10797 (2013).
18. Holby, E. F. & Taylor, C. D. Control of graphene nanoribbon vacancies by Fe and N dopants: Implications for catalysis. *Applied Physics Letters* **101**, 064102 (2012).
19. Holby, E. F., Wu, G., Zelenay, P. & Taylor, C. D. Metropolis Monte Carlo Search for Non-Precious Metal Catalyst Active Site Candidates. *ECS Transactions* **50**, 1839–1845 (2012).
20. Holby, E. F., Wu, G., Zelenay, P. & Taylor, C. D. Structure of Fe-Nx-C Defects in Oxygen Reduction Reaction Catalysts from First-Principles Modeling. *The Journal of Physical Chemistry C* **118**, 14388–14393 (2014).
21. Yeager, E. Dioxygen Electrocatalysis: Mechanisms in Relation to the Catalyst Structure. *Journal of Molecular Catalysis* **38**, 5–25 (1986).
22. Ramaswamy, N. & Mukerjee, S. Fundamental Mechanistic Understanding of Electrocatalysis of Oxygen Reduction on Pt and Non-Pt Surfaces: Acid versus Alkaline Media. *Advances in Physical Chemistry* **2012**, 17 (2012).
23. Tributsch, H., Koslowski, U. I. & Dorbandt, I. Experimental and theoretical modeling of Fe-, Co-, Cu-, Mn-based electrocatalysts for oxygen reduction. *Electrochimica Acta* **53**, 2198–2209 (2008).
24. Kresse, G. & Hafner, J. Ab initio molecular dynamics for liquid metals. *Physical Review B* **47**, 558–561 (1993).
25. Kresse, G. & Hafner, J. Ab initio molecular-dynamics simulation of the liquid-metal famorphous-semiconductor transition in germanium. *Physical Review B* **49**, 14251–14269 (1994).
26. Kresse, G. & Furthmuller, J. Efficiency of ab-initio total energy calculations for metals and semiconductors using a plane-wave basis set. *Computational Materials Science* **6**, 15–50 (1996).
27. Kresse, G. & Furthmuller, J. Efficient iterative schemes for ab initio total-energy calculations using a plane-wave basis set. *Physical Review B (Condensed Matter)* **54**, 11169–11186 (1996).
28. Perdew, J. P., Burke, K. & Ernzerhof, M. Generalized Gradient Approximation Made Simple. *Physical Review Letters* **77**, 3865–3868 (1996).
29. Perdew, J. P., Burke, K. & Ernzerhof, M. Generalized Gradient Approximation Made Simple [*Phys. Rev. Lett.* **77**, 3865 (1996)]. *Physical Review Letters* **78**, 1396–1396 (1997).
30. Grimme, S. Semiempirical GGA-type density functional constructed with a long-range dispersion correction. *Journal of Computational Chemistry* **27**, 1787–1799 (2006).
31. Lyalin, A., Nakayama, A., Uosaki, K. & Taketsugu, T. Theoretical predictions for hexagonal BN based nanomaterials as electrocatalysts for the oxygen reduction reaction. *Physical Chemistry Chemical Physics* **15**, 2809–2820 (2013).
32. Anderson, A. B., Uddin, J. & Jinnouchi, R. Solvation and Zero-Point-Energy Effects on OH(ads) Reduction on Pt(111) Electrodes. *The Journal of Physical Chemistry C* **114**, 14946–14952 (2010).

Acknowledgments

The authors wish to thank the Los Alamos National Laboratory for funding under the Laboratory Directed Research and Development (LDRD) program and for institutional computing resources. Los Alamos National Laboratory is operated by Los Alamos National Security LLC for the National Nuclear Security Administration of the U.S. Department of Energy under contract DE-AC528-06NA25396.

Author contributions

C.T. and E.H. prepared the main manuscript. E.H. performed the DFT calculations and prepared Figures 1–4. All authors contributed to data analysis and reviewed the manuscript.

Additional information

Competing financial interests: The authors declare no competing financial interests.

How to cite this article: Holby, E.F. & Taylor, C.D. Activity of N-coordinated multi-metal-atom active site structures for Pt-free oxygen reduction reaction catalysis: Role of *OH ligands. *Sci. Rep.* **5**, 9286; DOI:10.1038/srep09286 (2015).